CMST 20(3) 101-108 (2014) DOI:10.12921/cmst.2014.20.03.101-108

Cost-Effective and Sufficiently Precise Integration Method Adapted to the FEM Calculations of Bone Tissue

K. Mazur*, **L. Dąbrowski****

Faculty of Mechanical Engineering, Gdansk University of Technology
Gabriela Narutowicza 11/12, 80-233 Gdańsk, Poland
*E-mail: *katarzyna.mazur@pg.gda.pl, **ldabrows@pg.gda.pl*

Received: 20 June 2014; revised: 30 October 2014; accepted: 03 November 2014; published online: 11 November 2014

Abstract: The technique of Young's modulus variation in the finite element is not spread in biomechanics. Our future goal is to adapt this technique to bone tissue strength calculations. The aim of this paper is to present the necessary studies of the element's integration method that takes into account changes in material properties. For research purposes, a virtual sample with the size and distribution of mechanical properties similar to these in a human femoral wall, was used. WinPython, an environment of Python programming language was used to perform simulations. Results with the proposed element were compared with ANSYS element PLANE42 (with constant Young modulus). The modeled sample was calculated with five different integration methods at five different mesh densities. Considered integration methods showed a very high correlation of results. Two-point Gauss Quadrature Rule proved to be the most advantageous. Results obtained by this method deviate only slightly from the pattern, while the computing time was significantly lower than others. Performed studies have shown that accuracy of the solution depends largely on the mesh density of the sample. Application of the simplest integration method in combination with four times coarser mesh density than in ANSYS with a standard component still allowed to obtain better results.

Key words: FEM, bone, variable Young's modulus

I. INTRODUCTION

The finite element method was developed for structural engineering. Development of science has allowed its use for calculations in other areas. The technique of Young's modulus variation in the finite element was presented for functional graded composites [1] and fracture mechanics [2]. Our study aimed to adapt this technique to the bone tissue strength calculations. The currently used bone calculation method means assignment of individual material properties such as Young's modulus (E) to each of the model's element. Subsequent modulus' values are assigned to the elements by reading the intensity of radiation absorption for each pixel in HU (Hounsfield units) the scale of CT images radiodensity; it corresponds to the amount of radiation that a given structure absorbed: the bigger the number, the more radiation it absorbs. Calculation is performed using formulas (1) and (2) [3, 4]. In cited papers authors assumed bone tissue as isotropic material.

$$\rho\left[\frac{\mathrm{g}}{\mathrm{cm}^3}\right] = \frac{0.63 \cdot \mathrm{HU} - 6.7}{1000} \tag{1}$$

$$E[\mathrm{MPa}] = 1904\rho^{1.64} \tag{2}$$

Such calculations method (one image pixel – one Young's modulus) and differences in HU values of neighboring pixels generate discontinuities between adjacent elements. Discontinuities of properties do not occur in reality and should be considered as an error of the method. The common solution of this problem is to interpolate the material data on a refined mesh. Such action, however, does not improve the results significantly and also increases the computational time [5].

Authors' proposition of solving this problem is the use of a finite element which has different Young's modulus values in its nodes in the calculations. The functions describing changes of these values are used to define the material properties of the elements used in strength calculations. The aim of this numerical experiment was to choose the most advantageous method for $\boldsymbol{BD}$ matrix integration ($\boldsymbol{BD}$ matrix is the result of multiplying three matrices: strain matrix $\boldsymbol{B}$, elasticity matrix $\boldsymbol{D}$ and the Jacobian matrix $\boldsymbol{J}$). As a result of integration in generalized coordinates s and t the element stiffness matrix is obtained:

$$\boldsymbol{k} = g \cdot \int_{-1}^{1} \int_{-1}^{1} \boldsymbol{B}^T \cdot \boldsymbol{D} \cdot \boldsymbol{B} \cdot |\boldsymbol{J}| \mathrm{d}s \, \mathrm{d}t \tag{3}$$

Calculations, modelling and graphs were made in Python programming language, using the WinPython distribution.

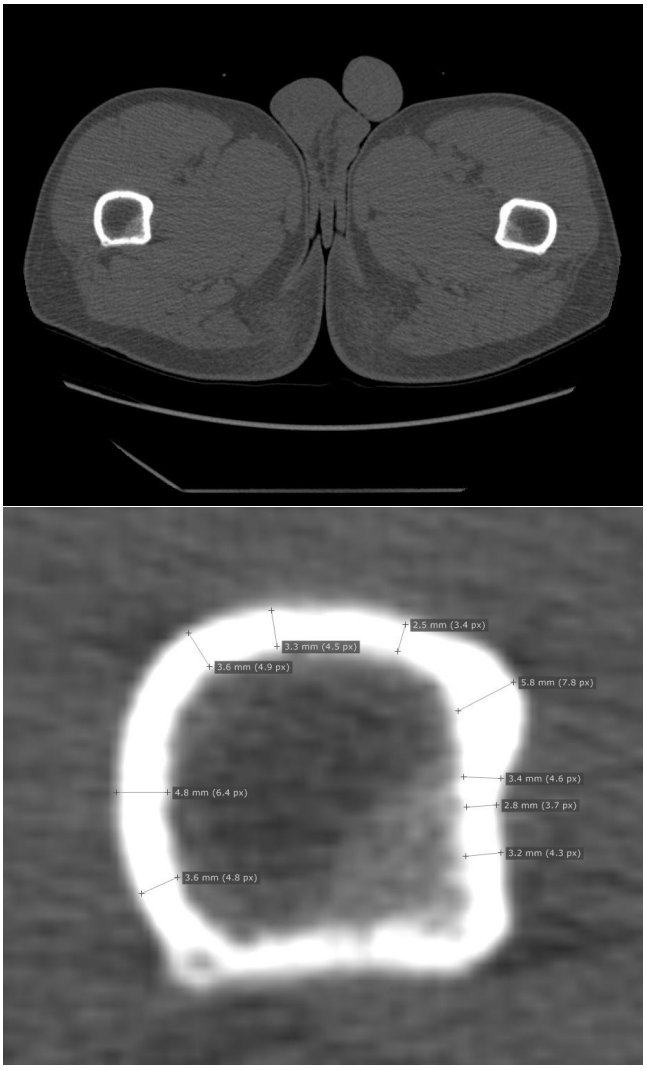

Fig. 1. Tomographic image of man's femur (top) and magnified view of the bone section (bottom)

II. MATERIAL AND METHODS

For the purposes of the numerical experiment quadratic model with dimension $l \times l = 1.3 \times 1.3$ mm and $g = 1$ mm thickness was created. Dimensions correspond to half of the human femur wall width (Fig. 1).

Young's modulus changes in the volume of the virtual sample according to its distribution in the bone: increases from the bone edge to the center of the wall and decreases again to the edge (Fig. 2). The computational experiment involves compression of the bone sample that has the same characteristics in every direction. The sample is supported on the lower edge (nodes from the bottom row could shift horizontally, except the node in point A which has both degrees of freedom removed) and loaded over the entire upper edge, and the side edges remain free. Compression is realized by the displacement of the upper nodes layer (kinematic constraint). The displacement value was calculated with the use of Hooke's law in one dimension (4). The displacement (Δl) value was chosen in such a way that, when Young's modulus for the entire sample is equal to the mean value $\overline{E}$ – generated the stress of 100 MPa [7]. Poisson ratio was set as 0.3 [8].

$$\Delta l = \frac{\sigma \cdot l}{\overline{E}} = -0.0967 \text{ mm}, \tag{4}$$

where $\sigma = 100$ MPa – compressive stress present in bone [7], $l = 1.3$ mm – height of the sample, $\overline{E}$ – mean value for Young's modulus $E_{\min} = 485$ MPa, $E_{\max} = 5377$ MPa, calculated with (1) and (2) for radiodensity of $700 \ldots 3000$ HU present in femur bone [7].

Our aim is the study of 2D Young's modulus problem before development of the 3D element. A plane stress model was selected for numerical methods study. The plane model is only a test and is not expected to be used in actual bone stress calculations. Its simplicity allows for clear visual inspection of the results. The test results in the next stage of work will be transferred to the 3D model. It was calculated using the standard 4-node rectangular element from the Serendipity family [9]. The shape function described the element in normalized coordinates is:

$$N_i = \frac{1}{4} (1 + s \cdot s_i) (1 + t \cdot t_i), \tag{5}$$

where $i = 0, \ldots, 3$ – node numbers, s_i, t_i – normalized coordinates at node i.

Each of the element's four nodes has two degrees of freedom: displacements along the x and y-axis. All elements have the same unitary thickness value. The material properties are assigned to the finite element by the elasticity matrix $\boldsymbol{D}$.

For plane stress state [6, 9]:

$$\begin{bmatrix} \sigma_x \\ \sigma_y \\ \tau_{xy} \end{bmatrix} = \boldsymbol{D} \cdot \begin{bmatrix} \varepsilon_x \\ \varepsilon_y \\ \gamma_{xy} \end{bmatrix} \tag{6}$$

$$\boldsymbol{D} = \frac{E}{1-\nu^2}\begin{bmatrix} 1 & \nu & 0 \\ \nu & 1 & 0 \\ 0 & 0 & \frac{1-\nu}{2} \end{bmatrix}, \tag{7}$$

where: ν – Poisson's ratio.

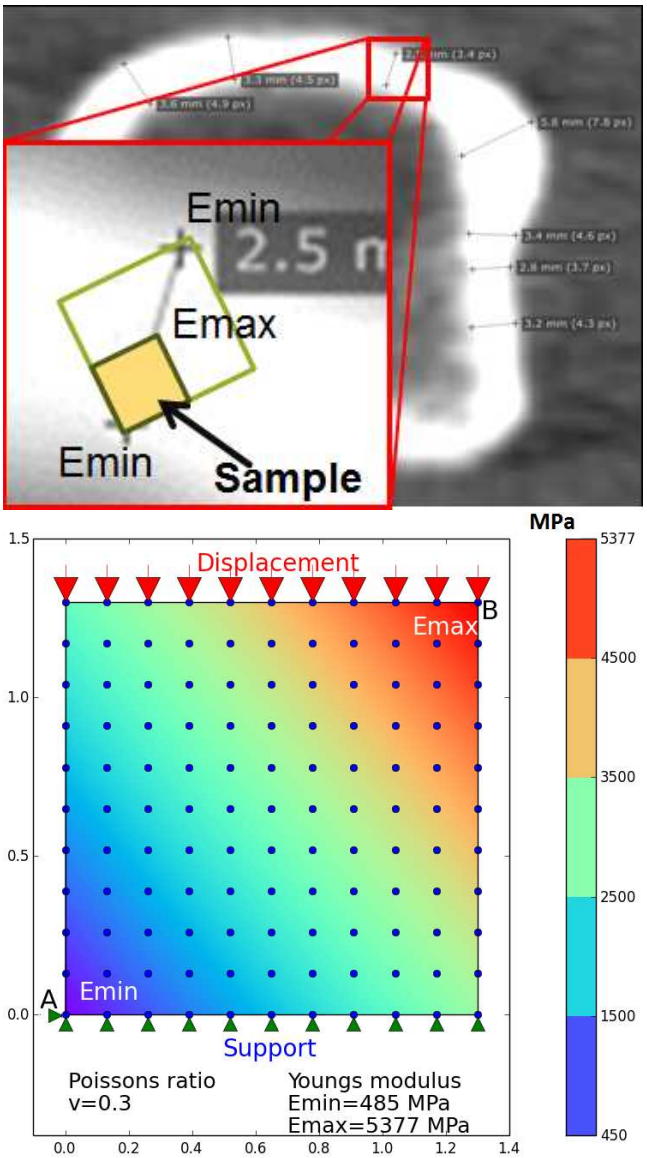

Fig. 2. Virtual sample and its place in bone area. Variability of Young's modulus from E_{min} to E_{max} was calculated by (1) and (2) for the common value of radiodensity on the shore and in the middle of the long bone's wall 700 . . . 3000 HU [7]. The distribution of E variation we simplified by linear distribution (8)

The plane stress model was used to perform calculations. An alternative would be the use of a plane strain model, but for testing numerical methods does not matter which method has been adopted. In addition, the plane stress model allows one to easily compare the results of compression for variable and constant E (the variation of the stress field depends only on variation of Young's modulus). In standard formulation of the single finite element, Young's modulus E is a single parameter defined as one value for the elasticity matrix. The authors' proposition is to write the Young's modulus parameter of a single finite element as a function dependent on x and y coordinates $E = E(x, y)$.

The finite element calculations are divided into two steps: the first one is to build the global stiffness matrix, while the second is calculation of displacements and stresses. Obtaining the global stiffness matrix is based on a summation of successive elements' local matrices. While creating the local stiffness matrix, for each of the elements' nodes Young's modulus value is calculated with the use of the formulae (8)

$$E_i = a \cdot x_i + b \cdot y_i + c, \tag{8}$$

where $i = 0, \ldots, 3$ – node numbers.

Then, the modulus value for a specific location are calculated on the element's surface according to the interpolation formula:

$$\begin{aligned} E =& E_0 \cdot \left(-\frac{s}{4} + \frac{1}{4}\right) \cdot (-t+1) + E_1 \cdot \left(\frac{s}{4} + \frac{1}{4}\right) \cdot \\ & (-t+1) + E_2 \cdot \left(\frac{s}{4} + \frac{1}{4}\right) \cdot (t+1) + E_3 \cdot \\ & \left(-\frac{s}{4} + \frac{1}{4}\right) \cdot (t+1), \end{aligned} \tag{9}$$

where s and t are natural coordinates of serendipity element [9]. As shown in (9), the modulus of the computed spot depends on the nodal modulus calculated with (8). Formula (9) is used to calculate the adequate values of Young's modulus for each of the $\boldsymbol{BD}$ matrix Gaussian integration points. This diversity of E in Gauss points is originality in FEM calculation for bone tissue (in classical FEM, value of E for each element's Gauss points are equal) – Fig. 3.

The additional variability introduced into the element raises the degree of a polynomial contained in the $\boldsymbol{BD}$ matrix, hence the need for the search for a cost-effective and sufficiently precise integration method for a variable Young's modulus element.

III. RESULTS

The calculations of the described sample were performed for five mesh densities 3×3, 10×10, 25×25, 50×50 and 100×100 elements. In FEM, before summing local stiffness matrices in a global one, every local's entire has to be integral. The authors used two methods of integration:

1. Numerical integration, by the trapezoidal method in 21 intervals in each direction.
2. Gaussian quadrature, in 2, 3, 4 and 6 points' coordinates.

Results of all integration methods for sample mesh density of 10×10 elements are almost identical, therefore, a complete set of results is shown in Fig. 4, while in Fig. 5 and 6 there are only results for two extreme methods.

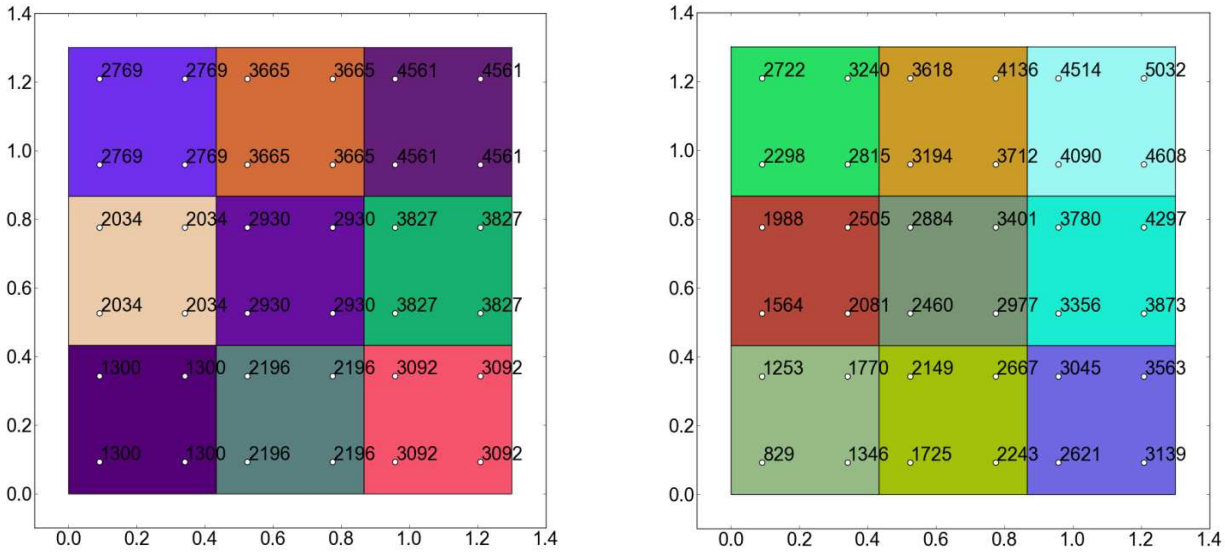

Fig. 3. Comparison of the Young's modulus values in the Gauss points for the classic FEM method (left) and with modifications used in this work (right)

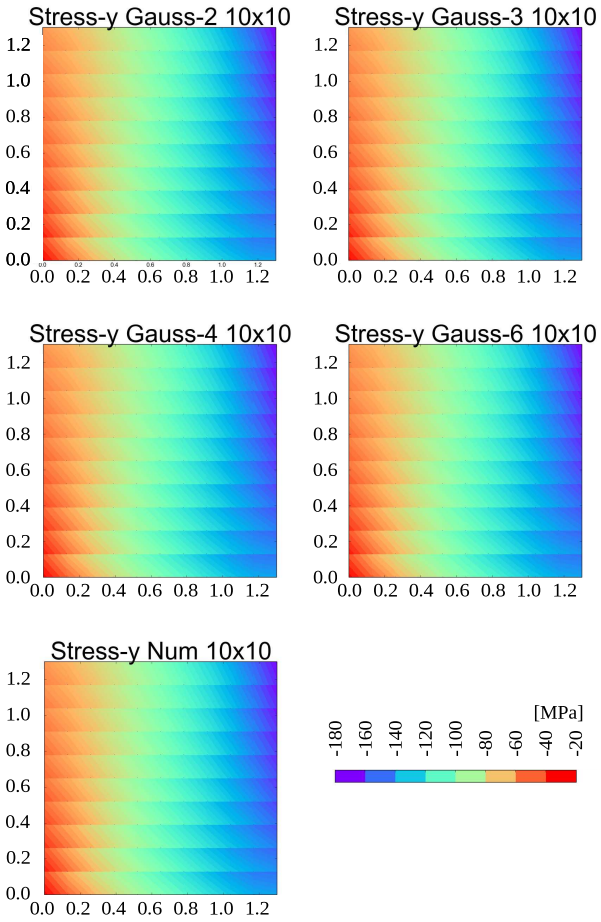

Fig. 4. Results of normal y stress calculations in 5 different integral methods with 10×10 meshing

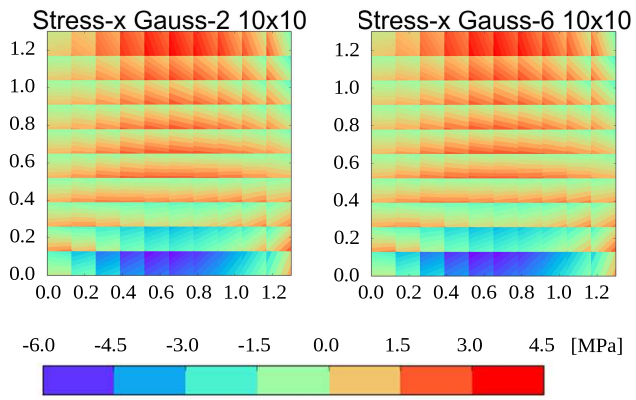

Fig. 5. Results of normal x stress calculations in 2 different integral methods with 10×10 meshing

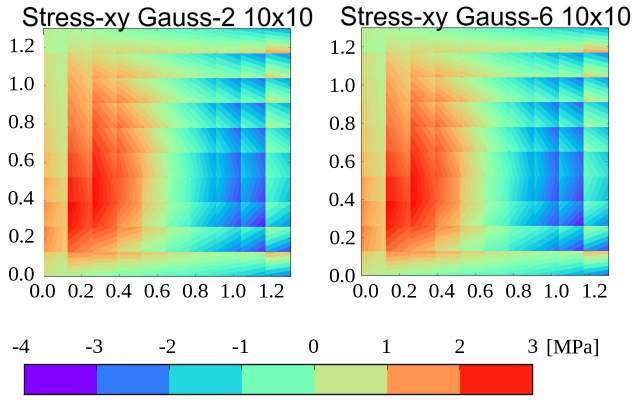

Fig. 6. Results of shear stress in xy plane calculations in 2 different integral methods with 10×10 meshing

To verify the accuracy of subsequent results graphs (Fig. 4-6) of the stress vs sample diagonal (Fig. 2 from A to B) coordinates were generated. In order to improve the accuracy of graphs (Fig. 7-10), stress was calculated for 3 additional points in every element. Discontinuity of stresses occurring between finite elements (stepped construction of the graphs Fig. 7-10) is a natural inaccuracy of FEM and is used to calculate indicator of calculation quality [9].

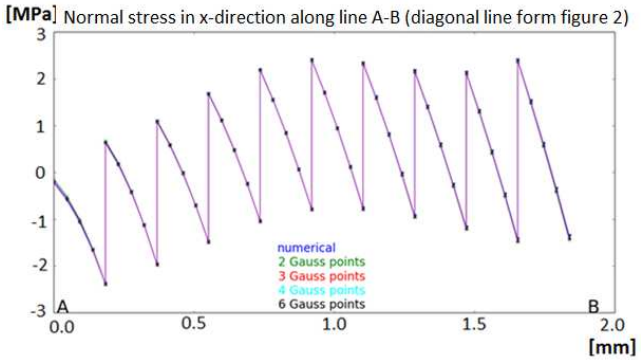

Fig. 7. Graph of stress on the distance on the diagonal AB for normal x-stresses

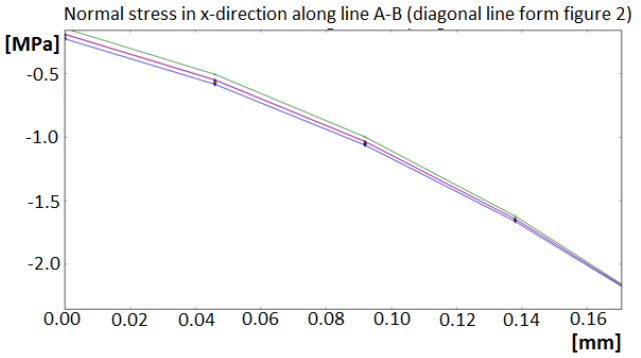

Fig. 8. First element (from the diagonal line) with the largest differences

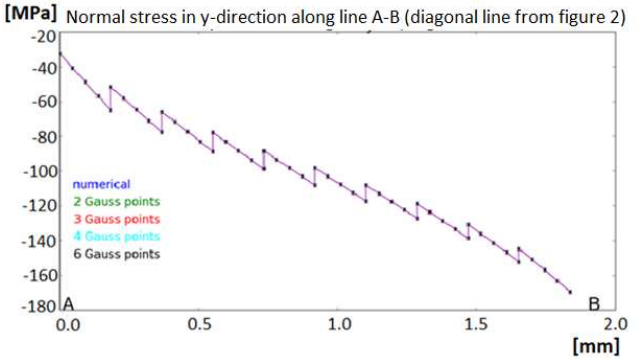

Fig. 9. Graph of stress on the distance on the diagonal AB for normal y-stresses

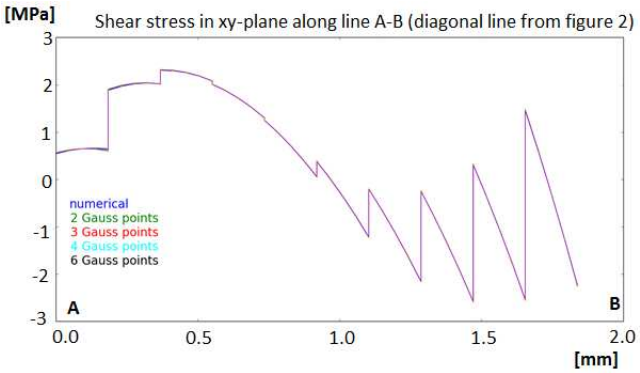

Fig. 10. Graph of stress on the distance on the diagonal AB for shear stress in xy plane

Differences between subsequent integration methods are nearly unnoticeable: less than 1%. Due to the satisfactory precision of the 2 Gauss point quadrature integration method, authors chose it to compare subsequent elements mesh density.

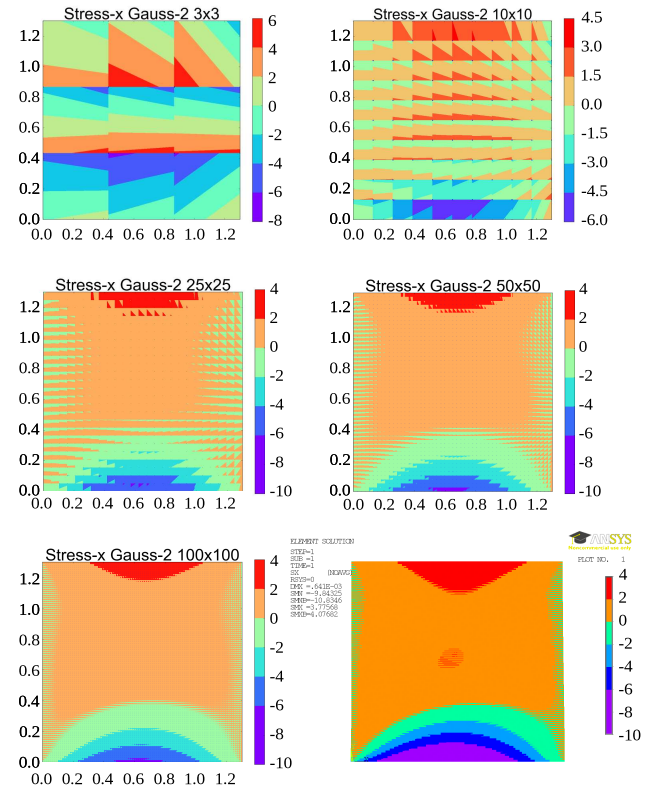

Fig. 11. Results of normal stress calculations in x-axis with various sample meshing (last picture calculated in ANSYS: one element one Young's modulus)

To verify the correctness of received results, calculations were performed with the ANSYS program. Comparison of results obtained with the authors' method and by ANSYS (Fig. 11-13) show nearly identical graphs, which proves that

element proposed by authors works correctly. Small differences in stresses' fields due to different calculation methods (our method: variable Young's modulus in element's volume, ANSYS: constant Young's modulus in element's volume) and various desktop environments.

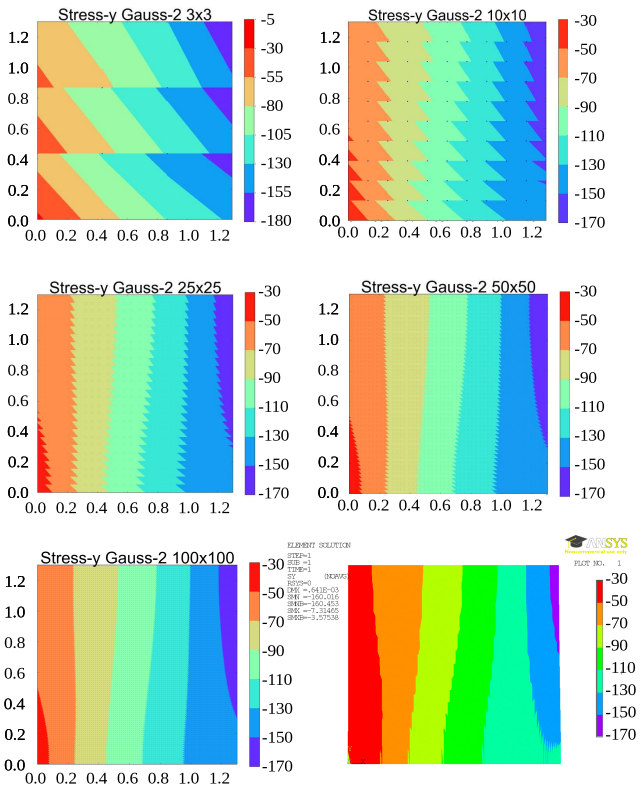

Fig. 12. Results of normal stress calculations in y-axis with various sample meshing (last picture calculated in ANSYS: one element one Young's modulus)

To compare results of stress calculations for the following meshing densities, graphs of the stress-sample diagonal coordinates (AB line), with like previous 3 extra points in every element were created (Fig. 14-16).

IV. DISCUSSION

Accuracy of calculation of normal stresses in the x-axis depends largely on the mesh density of the samples; the most accurate calculations were made with mesh density of 100×100 elements (Fig. 11-13). In the illustrated case, the force acts on the sample along the axis y, so the most convenient parameter is normal stresses at this very axis. Its very accurate results show that the division on just 25×25 elements, residual stresses require much less division of the same area. Mesh densities of 3×3, 10×10, 25×25 and 50×50 (Fig. 11-13) have nearly the same trend (Fig. 14). For x-axis stress sparse elements distribution (3×3) causes a shift of the calculated values in the sample area also it increases maximum stress values of 30%.

For y-axis (Fig. 15) stress we can observe the same dependence as for x-axis.

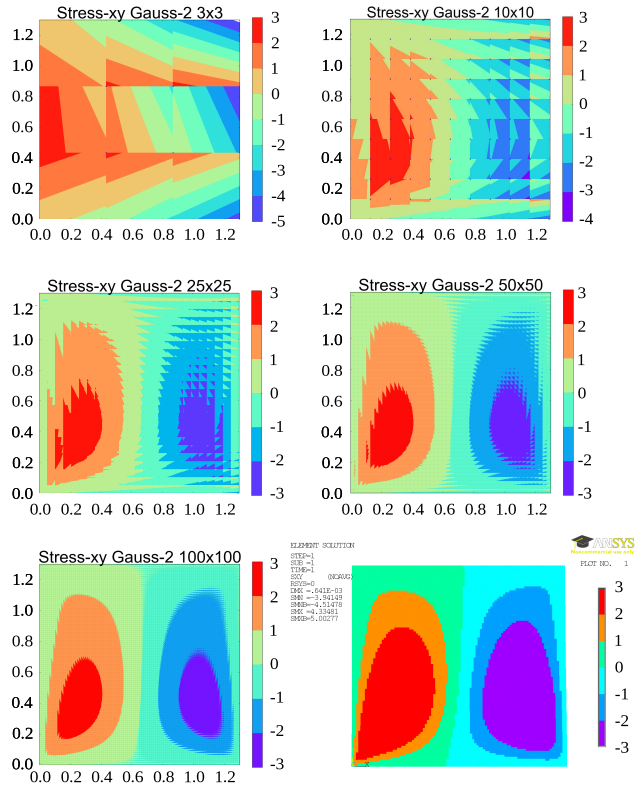

Fig. 13. Results of shear xy stress calculations with various sample meshing (last picture calculated in ANSYS: one element one Young's modulus)

The shear stress calculation (Fig. 16) shows significantly different results. Differences of calculated stress values have no systematic error.

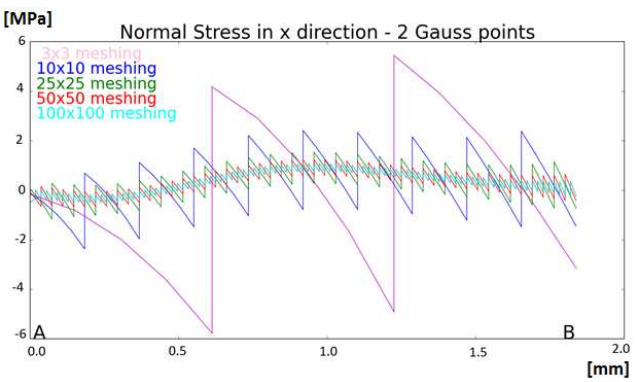

Fig. 14. Graph of stress on the distance on the diagonal AB for normal x-stresses. Different meshing, the same 2 Gauss points integration method

Tab. 1. Sample computing time by various integration methods (in seconds)

Method	Meshing 3×3	Meshing 10×10	Meshing 25×25	Meshing 50×50	Meshing 100×100
2 Gauss points	0.6472049	2.1001356	12.0611346	54.5561081	420.8379792
3 Gauss points	0.6782838	2.1776570	12.6584298	57.1105987	437.7866906
4 Gauss points	0.6893282	2.3199014	13.4893099	59.6273304	446.0396503
6 Gauss points	0.7374736	2.6436009	15.4095962	73.6180064	470.7408321
Numerical	0.6885902	2.2669395	13.3021994	66.6352694	460.9023881

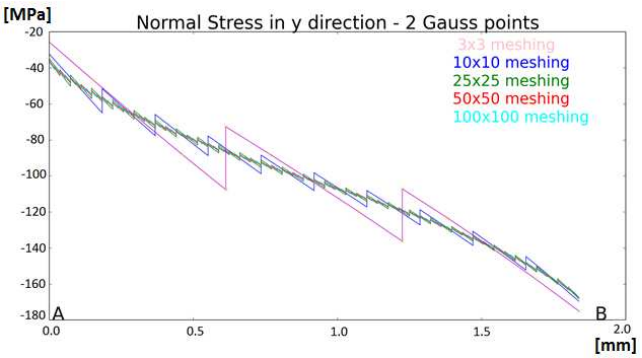

Fig. 15. Graph of stress on the distance on the diagonal AB for normal y-stresses. Different meshing, the same 2 Gauss points integration method

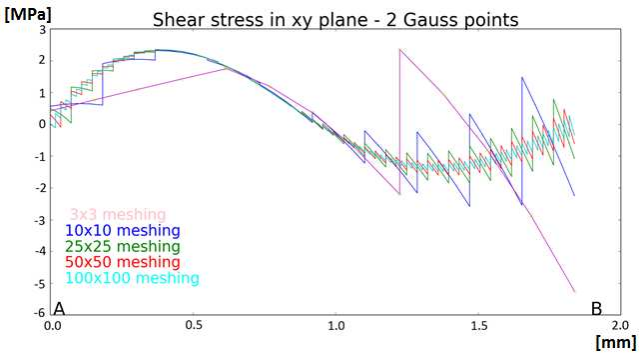

Fig. 16. Graph of stress on the distance on the diagonal AB for shear stress in xy plane. Different meshing, the same 2 Gauss points integration method

V. CONCLUSION

Despite raising the degree of a polynomial in the $\boldsymbol{BD}$ matrix in the finite element with varying Young's modulus, presented results clearly show that the two-coordinate Gauss quadrature integration method is sufficiently accurate, thus satisfactory and at the same time the fastest one (Tab. 1). In practice of the long bones CT images the pixel size should not be smaller than 1 mm due to the reduced radiation dose. The conducted studies show that with a 4-node finite element with size transferred directly from the CT scan and the Young's modulus gradient common in the thickness of the long bones, satisfactory results can be obtained only when the density distribution of the sample is increased to 25, which requires a CT pixel size of 0.052 mm and is both inaccessible and unacceptable. Therefore, one cannot count on accurate results of the calculations despite taking into account the Young's modulus component variability. Our further work will aim to consider the variability of Young's modulus in the 8-node finite element.

References

[1] J-H. Kim, G. H. Paulino, *Isoparametric Graded Finite Elements for Nonhomogeneous Isotropic and Orthotropic*, Journal of Applied Mechanics **69**(4), 502-514 (2002).

[2] J-H. Kim, G. H. Paulino, *T-stress in orthotropic functionally graded materials: Lekhnitskii and Stroh formalisms*, International Journal of Fracture **126**(4), 345-384 (2004).

[3] L. Grassi, E. Schileo, F. Taddei, L. Zani, M. Juszczyk, L. Cristofolini, M. Viceconti, Accuracy of finite element predictions in sideways load configurations for the proximal human femur, Journal of Biomechanics **45**(2), 394-399 (2012).

[4] R. Fedida, Z. Yosibash, Ch. Milgrom, L. Joskowicz, Femur mechanical stimulation using high-order FE analysis with continuous mechanical properties, II International Conference on Computational Bioengineering (2005).

[5] K. Mazur, L. Dąbrowski, *Young's Modulus Distribution In The Fem Models Of Bone Tissue*, National Conference on Applications of Mathematics in Biology and Medicine (2013).

[6] E. Błazik-Borowa, J. Podgórski, *Introduction to the finite element method in static of engineering structures*, IZT, Lublin 2001.

[7] W.P. Martins, *Questionable value of absolute mean gray value for clinical practice*, Ultrasound in Obstetrics & Gynecology **41**(5), 595-597 (2013).

[8] D.Ch. Wirtz, N. Schiffers, T. Pandorf, K. Radermacher, D. Weichert, R. Forst, *Critical evaluation of known bone material properties to realize anisotropic FE-simulation of the proximal femur*, Journal of Biomechanics **33**(10), 1325-1330 (2000).

[9] O.C. Zienkiewicz, R.L. Taylor, *The Finite Element Method*, Butterworth-Heinemann, Oxford 2000.

Katarzyna Mazur is a PhD student at Gdansk University of Technology, the Department of Mechanical Engineering. She received her MSc degree in Mechanical-Medical Science in 2012. Her ongoing thesis comprises FEM, CT data processing and programming.

Leszek Dąbrowski Senior Lecturer in the Chair of Machine Design and Automotive Engineering in the Department of Mechanical Engineering in Gdansk University of Technology. He graduated in 1985 and obtained PhD in mechanical engineering, specializing in the field of tribology in 1997. His scientifical interests also include computational methods in engineering, biomechanics, medical engineering. His recent work focuses on the use of CT data in FEM and its application in orthopedics and dentistry.

 DOI:10.12921/cmst.2014.20.03.101-108